Asian Journal of Physics
Vol. 31, Nos 3 - 6 (2022) 515-530
Available on: www.asianjournalofphysics.com

ap

Simulation and analysis of light scattering from particulate matter: A review

Kalpak Gupta and M R Shenoy

Department of Physics, Indian Institute of Technology Delhi, New Delhi – 110 016, India

Dedicated to Professor Bishnu P Pal for his enormous contributions to the advancement of research and education in science and technology through his unique vision and outstanding dedication

Light scattering techniques are ubiquitous and essential components of many methodologies which require the non-invasive characterization of particulate matter. Here, we present an overview of various methods which are usually used to calculate the characteristics of the light scattered by such media. The scattering problem—the objective of which is to obtain the properties of the scattered light relative to the incident light for a given type of particle—can be modelled in the form of a boundary value problem, and it can be solved through different analytical and numerical techniques. The discussion is then extended to the description of light propagation in turbid media, which is of importance in several practical applications. A turbid media consists of suspended particulate matter, which often leads to multiple scattering of light, further complicating the solution of the scattering problem. We outline both analytical and numerical techniques for solving the scattering problem, with particular focus on the Mie theory and the Monte Carlo method with examples. Finally, we conclude with a brief discussion on some of the neoteric applications of light scattering studies.

Keywords: Light scattering, Scattering theory, Particulate matter, Turbid media, Monte Carlo simulation.

1 Introduction

Particulate matter, i.e., a medium with particles of very small dimensions, is a ubiquitous part of our everyday environment. In turbid liquids, it primarily refers to suspended particles, which can be sediments present in water bodies, such as clay, sand, silt, etc. [1-3], artificial man-made waste particles, such as polymers, which are harmful in large quantities, and even biological specimens such as algae, which plays a pivotal role in various ecosystems. Particulate matter is also found in air in the form of pollens [4], pollutants [5,6], and aerosols [7,8]. In most applications, it is not a single particle but a collection of particles in a medium which needs to be analyzed—such media which consist of suspended particles are called turbid media [9–11]. Detection and characterization of the various types of particulate matter are of utmost importance in several applications, ranging from monitoring of air pollution [12] and pollen concentration [13], to determination of turbidity of potable water [14-16], and monitoring pollutants in wastewater [17,18]. Thus, a panoply of particulate matter with various shapes and sizes exists in nature, and a variety of methods are employed to study such particles; examples of such methods are mass spectrometry, gravimetric method and microscopy.

Currently, light scattering techniques are widely used for the characterization of particulate matter [19-23], such as for detection of particles [24], determination of particle size [25,26], and estimating concentration of sediments in water bodies [1,3,27]. This is augmented by its several advantages [3] like non-invasive nature, real-time results, and scope of telemetry using optical fibers [27,28]. When light is incident on particulate matter, it interacts in the form of scattering and absorption [Fig 1(a)]. The properties

Corresponding author
e mail: kalpakgupta@physics.iitd.ac.in (Kalpak Gupta)

of the scattered light, such as the total amount of scattered light and the angular distribution of the scattered light intensity, depend on the properties like shape, size, and refractive index of the scattering particle. Thus, from measurement of the scattered light, the properties of the suspended particles can be determined, which is called the inverse scattering problem [29,30]. However, there is a caveat: The property of a particle usually refers to its physical boundaries like shape and size, which can be obtained through some form of imaging, and also composition, which can be determined using chemical methods. In contrast, in the case of light-matter interaction, the particle is defined by parameters such as the extinction cross section and the phase function, which depend on the properties of the particle [31-33]. The total (extinction) cross section C_t is defined as the ratio of the total scattered (and absorbed) power to the incident intensity, and has units of area. It is the sum of the scattering cross section C_s and the absorption cross section C_a, which are the ratios of the scattered light– and the absorbed light power, respectively, to the incident intensity. The phase function $p(\theta, \phi)$ dictates the amount of light scattered in a particular direction, where 'direction' is defined by the scattering angle θ and the azimuthal angle ϕ [Fig 1(b)]. The aforementioned parameters depend on the physical properties of the particles. Therefore, in light scattering studies, the aim is the determination of these parameters in order to characterize the physical properties of a given type of particulate matter.

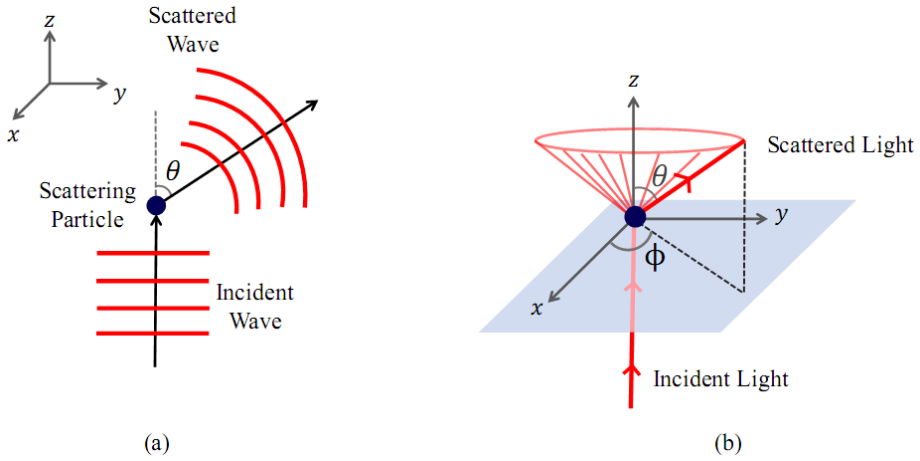

Fig 1. (a) A plane polarized wave is incident on a particle, and is scattered at angle θ. The two arrows in different directions represent the propagation vectors. The z-axis is fixed to be the direction of the incident light, with the position of the scattering particle as the origin. (b) There can be many directions of the scattered light corresponding to a particular value of the scattering angle θ; these different directions form a cone around the z-axis (the wavefronts are not shown here). The direction is uniquely determined by the azimuthal angle ϕ in addition to θ, where ϕ is the angle between the x-axis and the projection of the propagation vector of the scattered wave on the x-y plane.

In the case of a turbid medium, the propagation of light is described in terms of some scattering parameters, such as the interaction coefficient μ_t, the albedo b, and the anisotropy parameter g [10,11,34, 35]. The interaction coefficient μ_t is the probability that light interacts (through scattering and absorption) with a particle per unit infinitesimal path length while propagating inside the turbid medium. μ_t is the sum of the scattering coefficient μ_s and the absorption coefficient μ_a, which are defined similarly. The inverse of μ_t is the mean free path of light between two interaction events when it is propagating in the turbid medium. The interaction coefficient can also be expressed as the product of the cross section C_t and n, which is the concentration of particles in the medium [31]. The albedo b, which is the ratio of μ_s and μ_t, describes the amount of absorption by the medium. The value of b ranges from 0 to 1, which corresponds to purely absorbing (with no scattering) and non-absorbing media, respectively. The anisotropy parameter g is the average of cosine of all the scattering angles corresponding to the scattering events in the medium. g can be

calculated from the phase function $p(\theta)$; here the dependence of the phase function on ϕ has been dropped by assuming azimuthally symmetric scattering, which is usually the case. The value of g ranges from –1 to 1, which refers to the respective cases of complete backscattering ($\theta = 180°$) and complete forward scattering ($\theta = 0°$); $g = 0$, corresponds to the case of isotropic scattering. Thus, the inverse problem encompasses the determination of these scattering parameters, since they depend on the properties of the constituent particles of the turbid medium.

The general methodology to determine the properties of particulate matter from light scattering measurements is as follows: If the scattered light corresponding to a large range of scattering angles is measured, then first the cross section of the particle is determined from the measurement at the 0° scattering angle by using the optical theorem, and then the phase function can be obtained from the angular spectrum of the scattered light intensity. Once C_t, C_a, and $p(\theta)$ are determined, there is still a need to determine the actual physical properties of the particle, which are the shape, size, and the refractive index profile (which depends on the particle composition). To achieve this, the scattered light corresponding to different possible particle characteristics can be calculated and compared to the experimentally obtained parameters [36,37]. While using this methodology of comparing the results with a theoretical value of the scattered power corresponding to different particle properties, sometimes it is possible to decrease the angular resolution of the measurements or even restrict the number of measurements to only one or two, such as in the case of flow cytometry [38-40].

For a turbid medium, the analysis is similar, but involves measurement of the unscattered light from the sample, from which μ_t is obtained by using the Beer-Lambert law [10,11,33]. Then, $p(\theta)$ or g is determined from the measurements of the scattered light; this can be achieved either from empirical formulae or calibration curves, both of which relate the scattered light to one or more scattering parameters [10,11,35,41]. Though it is possible to obtain such relations by performing experiments with a wide variety of samples, it is prudent and facile to obtain these from analytical calculations or numerical simulations. Thus, calculation and simulation of light scattering from a particle or a group of particles is indispensable for determination of the particle properties. In addition to intensity measurements, polarization gating can be used to perform Mueller matrix polarimetry, which studies the relation between the Stokes parameters of the incident light and the scattered light, to obtain further information about the particle(s) [42-46]. Again, in such cases, it is essential to calculate the light scattering characteristics of a particle or a turbid medium, to relate the Mueller matrix and the actual properties of the scatterers.

In this review, we discuss some of the methods widely reported in the literature which can be used to calculate, simulate, and analyze light scattering from particulate matter. In Sec 2, we focus our discussion on light scattering from single particles, and then in Sec 3, we extend our discussion to the case of turbid media, which is a much more prevalent object of study when it comes to practical applications. Finally, we present the conclusions in Sec 4.

2 Single Particles

The *scattering problem* comprises finding the properties of the scattered light, corresponding to the incident light, for a given type of particle [31]. The solution of the scattering problem primarily refers to the amplitude scattering matrix, which relates the scattered light to the incident light for both types of polarization (parallel and perpendicular). As discussed above, if the light is defined in terms of the Stokes parameters, then the Mueller matrix is used instead of the scattering matrix. It is from this scattering matrix that the parameters such as the extinction cross section and the phase function can be obtained. In Secs 2.1 and 2.2, we detail a few commonly used analytical and numerical methods of obtaining the properties of the scattered light from a single particle. A similar discussion pertaining to the case of turbid media is given in Sec 3.

2.1 Analytical Methods

The scattering problem is essentially a boundary value problem due to the different values of the refractive indices inside and outside the particle, and it can be solved using the Maxwell's equations. Apart from the occasionally lengthy calculations, the scattering problem is a direct problem, which can be uniquely solved if all the boundary conditions are known [29]. In simple cases, such as for spheres and spheroids, the solutions can be obtained analytically. The Mie theory [31,47], for example, gives the analytical solution for spherical particles. A rigorous derivation of the Mie theory can be found elsewhere [31,32,34]. We explain in brief the salient steps for obtaining the solutions: From the Maxwell's equations, the vector wave equation is obtained, whose solutions are in the form of spherical harmonics. The incident wave, the scattered wave, and the internal wave inside the particle are expanded in terms of the spherical harmonic solutions, and their expansion coefficients are related in terms of the Mie coefficients. The Mie coefficients are calculated from the boundary conditions, i.e., the tangential components of the electric– and magnetic fields are continuous at the boundary defining the scattering particle. Since both the incident wave and the Mie coefficients are now known, the scattered wave can be calculated, from which the cross sections and the phase function can be obtained. The Mie coefficients depend only on the size parameter χ and the relative refractive index n_r for a given scattering system (particle-medium combination). χ is the ratio of the circumference of the particle and the wavelength of light in the surrounding medium, and n_r is the ratio of the refractive index of the particle to that of the medium. The significance of these parameters in Mie theory is that for a given pair of χ and n_r, the calculated cross sections and the phase function are the same, irrespective of the individual properties of the particle (and medium).

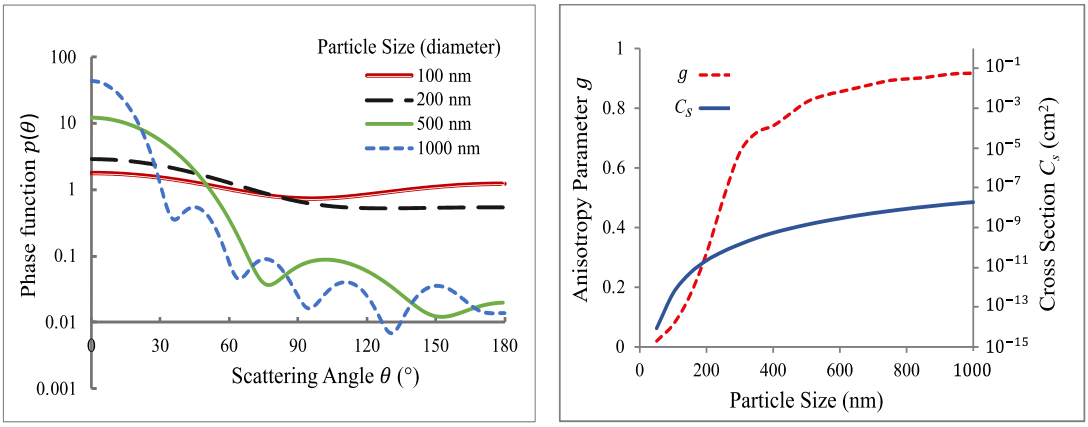

(a) (b)

Fig 2. (a) The Mie phase function (for unpolarised light) for four different sizes of polystyrene spheres, corresponding to the wavelength $\lambda_0 = 632.8$ nm. (b) The anisotropy parameter g and the scattering cross section C_s corresponding to each particle size, calculated using the Mie theory. Since polystyrene is non-absorbing at λ_0, $C_s = C_t$, the total cross section, in this case.

Since the fields in the solution of the Mie theory are expressed as infinite series of spherical harmonics, the accuracy is higher if a higher number of terms are used for the calculations. Earlier, the calculations used to be cumbersome, but with the advent of computer processing power and improvements in the algorithms [48], many softwares/programs have become available [32,34,49] to obtain numerical solutions. Thus, corresponding to the size and the refractive index of a given spherical particle, the scattering characteristics of the particle can be obtained from the Mie theory. For example, suspensions comprising polystyrene microspheres (latex beads) are often used as standard samples in scattering experiments; Fig 2

shows the values of the phase function, the cross section, and the anisotropy parameter for polystyrene spheres of different sizes dispersed in water, corresponding to the wavelength $\lambda_0 = 632.8$ nm. The calculations were performed using the *MiePlot* software by Philip Laven [49]; for the calculations, the refractive indices of the particle and the medium were taken to be 1.587 [50] and 1.3317 [51], respectively. It can be seen from Fig 2 that as the particle size increases, the phase function becomes more and more oscillatory and anisotropic, leading to an increase in the probability of forward scattering; this is a well-known feature of the Mie theory.

The Mie theory is one of the commonly used scattering theories due to its relatively simpler derivation and ease of analysis, and it has a wide scope of applicability due to the prevalence of spherical particles in nature. Although it is impeccably valid for spherical particles, many features of the Mie theory are in fact also valid for non-spherical particles, especially when the size is small, in which case the particles are treated as spherical with an equivalent or average radius [52,53]. The Mie theory can also be applied to nearly-spherical particles through the use of first-order perturbations [54]. In the past few decades since the Mie theory was first proposed, extensions of the theory for the cases of coated spheres [55,56], chiral spheres [57], i.e. particles in which the two different circular polarizations experience different refractive indices, spheres with a radial refractive index gradient [58], and even charged dielectric spheres [59] have been reported. A history of some of these theories can be found in [60]. Analytical solutions have also been reported for the case when the medium surrounding the spherical particle is absorbing [61], as well as for spheroids and cylinders, including coated particles. In these cases, the solutions can be obtained by following a separation of variables approach similar to the Mie theory, albeit with an (expected) increase in the complexity [32,62,63].

If the particles are of irregular shape, or if an analytical solution cannot be obtained directly, it is sometimes possible to estimate the scattering characteristics of a particle using suitable approximations. The Mie theory is useful for particles with size larger than or comparable to the wavelength of the incident light, in which case the light scattered from different parts of the particle interfere, giving rise to an oscillatory phase function. On the contrary, in case the particle is much smaller than the wavelength of light, the scattering particle can be treated as an oscillating dipole driven by the incident field—at any given moment, the electric field is assumed to be constant throughout the particle. Under this approximation, called the Rayleigh scattering approximation [31,34,64], the calculated scattering cross section depends on the polarizability of the particle, and is inversely proportional to the fourth power of the wavelength, which provides a well-known explanation for the blue colour of the sky during the day and the orange-red colour at sunset or sunrise. In Rayleigh scattering, the perpendicular component of the scattered light is isotropic, while the parallel component scatters almost isotropically. This is also corroborated by Fig 2, where it can be seen that the scattering is almost isotropic for particles of small size, which is the valid regime of the Rayleigh approximation.

Approximations such as the Rayleigh theory are useful because they simplify the procedure of obtaining the solutions, or at the very least, provide insights into the scattering characteristics without going through a complicated (and often computationally intensive) procedure. For instance, the difference in the results of the Mie theory and the Rayleigh theory reduces drastically as the particle size decreases, although the Mie theory is an exact solution, whereas the Rayleigh theory is an approximation. Another example of such approximation is the Rayleigh-Gans theory, which is applicable to optically soft particles [31,32]. In the Rayleigh-Gans theory, the internal field inside the particle is approximated to be equal to the incident field; an interesting example of its application is the analysis of scattering by cylindrical particles [32]. Approximate analyses can also be performed for particles very large compared to the wavelength of light, by incorporating interference and diffraction based on the Huygen's principle, or through geometric ray tracing [65], which, for example, can be used to analyze the formation of rainbows from water droplets.

2.2 Numerical Methods

If the analytical solution for a given scattering problem is complicated, or if it is not possible to obtain one, numerical methods such as the finite-difference time-domain method (FDTD) [66-68] and the finite element method (FEM) [69] can be used. The FDTD method involves solving the time-dependent Maxwell's equations by dividing the scattering system into cubic or rectangular meshes, so the solutions are obtained at the discrete points forming a mesh. In the case of FEM, the analysis is applied on a time invariant system, and the size and shape of the meshes can be varied as required—for example, over a region where the fields vary slowly, the size of the mesh can be increased, which reduces the computation time.

The scattering problem can also be solved by using the volume integral equation, which is often used in the case of inhomogeneous particles. In this method, the particle is divided into many smaller particles, whose scattering properties are calculated by the methods such as the T-matrix method [70], the method of moments (MoM) [71], or the discrete dipole approximation (DDA) [72]. The T-matrix method [73-75] is especially useful for irregular (non-spherical) particles. In the T-matrix method, the incident and the scattered light are expressed in terms of spherical vector harmonics. The expansion coefficients of scattered field are related to the expansion coefficients of the incident field through the T-matrix, which is obtained by numerical integration over the surface of the particle while using the boundary conditions. This is similar to the case of Mie theory, in which instead of the T-matrix, the solutions are analytically obtained in terms of the Mie coefficients. The T-matrix method can be used to obtain the Sh-matrix for a particular particle shape [76], which is independent of the size and refractive index of the particle, and thus offers additional advantages. The solution of the scattering problem has also been reported for spheroids using the T-matrix method [77]. A detailed review about the T-matrix method can be found in [78].

The MoM [79] uses surface integrals obtained from operator equations, which are converted into a system of linear equations expressed in the form of a matrix, whereas in the DDA [80], the particle is modelled as a cubic assembly of interacting dipoles. Thus, there are several methods to solve the scattering problem numerically, all of which involve the solution of the electromagnetic equations in some form. It should be noted that sometimes the scope of application of a numerical method is dependent on the properties of the scattering system, since the values of various parameters may affect the existence, convergence, and uniqueness of the solutions. The choice of the method also depends on the available computational resources, the precision required, and the time taken for the calculations; these factors dictate the suitability of a chosen method in the context of a given type of particle.

3 Multiple Particles: Turbid Media

For a collection of stationary particles, the methods described in Sec 2 can be suitably extended to obtain the properties of the scattered light by using appropriate boundary conditions [60]. In contrast, a turbid medium comprises a large number of suspended particles that are undergoing random motion in the medium. Such a medium is characterized by the probability of light being scattered at different positions inside the medium; this probability depends on the scattering parameters, which further depend on the properties and the concentration of the particles present in the medium. In this section, we give some of the methods to describe the propagation of light inside a turbid (scattering) medium.

3.1 Analytical Models and Approximations

There exist several methods to model the propagation of light inside a turbid medium. The simplest one is the random-walk model, in which the scattering *particles* (discrete points where light undergoes scattering) are situated in a cubic grid, and the scattering can be either isotropic [81] or anisotropic [82]. The random-walk model can be further modified to include the effect of polarization [83] and inhomogeneity in the medium, i.e., when the turbid medium consists of non-scattering regions [84]; in these cases the

particles are often positioned randomly instead of in a static grid, leading to stochastic modelling (see Sec. 3.2). It is also possible to consider the probability of light being scattered continuously while propagating inside the medium. This is the basis of the radiative transfer equation (RTE) [34,85], which is based on the conservation of energy and describes the radiance (energy flow) inside the turbid medium. The RTE can be arrived at by considering the various sources of extinction and generation of light within a given volume of the turbid medium [34]. The loss of energy inside the volume is due to scattering and absorption of light, while the positive contribution is due to generation of energy by a source (if any) within the volume and due to light scattered from other particles into the volume. Note that the light intensity inside the volume under consideration may also increase or decrease due to the convergence or divergence of the beam of light propagating through the volume.

Although the RTE is an analytical equation, it is difficult to solve rigorously, and thus the corresponding diffusion approximation is often used [34,81,86]. The diffusion approximation is applicable to highly scattering media, and is obtained by expanding the radiance in terms of zeroth and first order spherical harmonics [34]; it has been reportedly applied to highly absorbing media as well [87]. The expansion of the radiance may be carried out up to a higher order N to obtain the P_N approximation, where the value of N is chosen according to the desired accuracy and computation time [88,89]. Under the diffusion approximation, the distribution of light energy inside the medium is almost isotropic and is dependent on μ_a and μ_s', which is the reduced scattering coefficient; μ_s' can be expressed in terms of μ_s and g as $\mu_s' = \mu_s(1-g)$. The inverse of μ_s' is the transport mean free path, which is the average distance a photon will move along its original direction after undergoing an infinite (very large) number of scattering events. From the expression of μ_s', it can be seen that as μ_s increases or g decreases, the transport mean free path decreases, which is expected as the scattering becomes increasingly isotropic. Note that in many cases, it is prudent (and sometimes the only way) to obtain the solutions by solving the relevant equations numerically, even after suitable approximations have been applied.

3.2 Monte Carlo Method

The 'gold standard' for modelling of light propagation in a turbid medium is the Monte Carlo method [11,34,35,90,91], which in principle is equivalent to the RTE, but involves a stochastic methodology instead of analytical solutions. In Monte Carlo simulations, the propagation of light is represented by propagation of photon packets (energy packets), wherein each packet comprises hundreds or thousands of photons. In the simulations, a large number of photon packets are launched into the turbid medium; these packets propagate according to the medium's scattering parameters and a random variable ξ, which lies between 0 and 1. The packets travel inside the medium in straight line paths, and get scattered at the scattering angle θ and the azimuthal angle ϕ after each interaction (scattering event), with a step size s till the next interaction point [Fig 3(a)]. A weight is associated with each photon packet to take care of absorption in the medium, which is initially set to unity. In the presence of absorption, the weight of the packet is reduced to account for the loss of energy at the scattering site and between two successive scattering events [34,91]. The flux of the packets (per unit time) at a given position inside the turbid medium is equivalent to the intensity of the scattered wave at the same position. Note that the term *photon packet* refers to the light being treated as a collection of classical objects, such that simulations involving a large number of packets result in the same constitution as that of a wave propagating inside the scattering medium; there are no quantum effects involved in the model. As the number of simulated packets increases, the distribution of the scattered energy packets resembles the distribution of the scattered wave more accurately.

When a photon packet is propagating inside the turbid medium, the values of the variables θ, ϕ and s after each interaction are obtained through the use of the *inverse distribution method*, which maps the random number ξ to the variables according to their respective probability distributions, which in turn are expressed in terms of the scattering parameters of the medium [34]. Typically, the step size is given by $s = -\log(\xi)/\mu_t$,

and the scattering angle θ is obtained from a suitable phase function. The scattering is usually assumed to be azimuthally symmetric, so the azimuthal angle is simply $\phi = 2\pi\xi$. After the determination of s, θ and ϕ, the coordinates of the photon packet are updated as shown in Fig 3 (b). Each photon packet propagates independently, and is terminated if it exits the medium or reaches the detector. Once all the packets have been terminated, the total weight of all the packets collected at the detector divided by the number of photon packets incident on the medium is the fractional scattered power at the position of the detector, corresponding to the particular set of scattering parameters used for the simulation run.

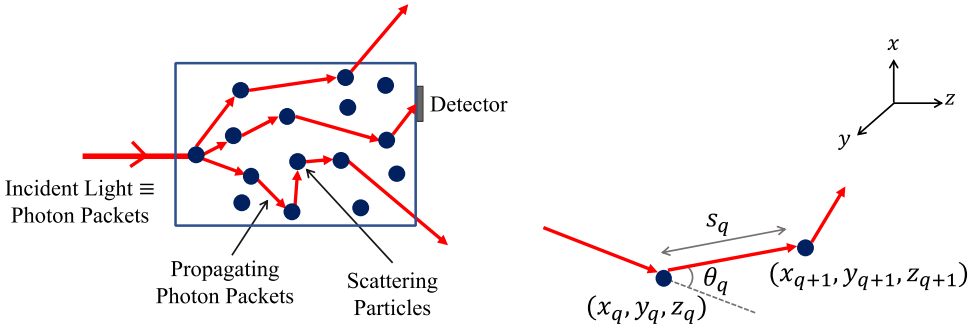

Fig 3. (a) Propagation of photon packets inside a turbid medium. The packets are initially launched in the direction of the incident light, which change their direction of propagation after each scattering event. The propagation of three different packets are shown in the figure, one of which reaches the detector. (b) A photon packet is scattered at (x_q, y_q, z_q), which is the position of the q^{th} interaction event, q is an integer. The scattering angle θ_q and the step size s_q after the q^{th} interaction are obtained from the scattering parameters and the random number ξ, and then the photon packet propagates to the position of the $(q+1)^{th}$ interaction. The azimuthal angle ϕ (not shown) is also incorporated if the model is three dimensional.

The phase function plays an important role in the simulation of different types of scattering media. As discussed in Sec 1, the phase function of a particle depends on its various parameters like shape, size, and refractive index, and it can be calculated after obtaining the solutions of the scattering problem for the given particle, either numerically or analytically (Sec 2). If the properties of particle are not known, which is expected in the case of practical turbid samples, then it may not be possible to obtain a numerical solution, even if the computational cost is condoned. In such cases, some pre-defined phase functions may be used for the simulations. Some of the commonly used phase functions reported in the literature are the Henyey-Greenstein phase function [10,92], the modified Henyey-Greenstein phase function [93,94], the Reynolds-McCormick phase function [41,95] and the Mie phase function [11,94,96], among others [97]. For scattering from small particles, where Rayleigh scattering theory is applicable, the Rayleigh phase function can also be used [34,93].

The Henyey-Greenstein phase function was first proposed to describe the scattering of light from galactic dust [92], and has established itself as the most widely used phase function for simulation of light scattering, especially in the case of biological tissues [68,98]. This is facilitated by its simple and analytically invertible expression, even though it has limited accuracy in some cases [11,41]. The Henyey-Greenstein phase function is expressed in terms of the anisotropy parameter g as follows [91,94]:

$$p(\cos\theta) = \frac{1}{2}\frac{(1-g^2)}{(1+g^2-2g\cos\theta)^{3/2}} \tag{1}$$

The application of the inverse distribution method gives [91]

$$\cos\theta = \begin{cases} \dfrac{1}{2g}\left[1+g^2-\left(\dfrac{1-g^2}{1-g+2g\xi}\right)^2\right] & \text{for } g \neq 0 \\ 2\xi - 1 & \text{for } g = 0 \end{cases} \tag{2}$$

The Mie phase function, as its name implies, is best suited for simulation of light scattering from spherical particles [33,61,99], and can be obtained from the Mie Theory (Sec 2.1). The Mie phase function for a particular spherical scatterer is expressed as an infinite expansion of Legendre polynomials [100,101]; hence, it is not possible to invert it analytically, unlike in the case of the Henyey-Greenstein function. However, the inverse distribution method can still be used in a discrete form [11,94], by using look-up tables. Choosing the scattering angle after each interaction using look-up tables usually increases the calculation time while decreasing the accuracy; however, these issues can be mitigated by using interpolation techniques and equivalent analytical functions which approximately replicate the discretized phase function [102]. Sometimes, the aforementioned phase functions are not sufficient to describe the distribution of the scattered light from a particle; in such cases, a combination of different phase functions may be used for the determination of θ [103-105].

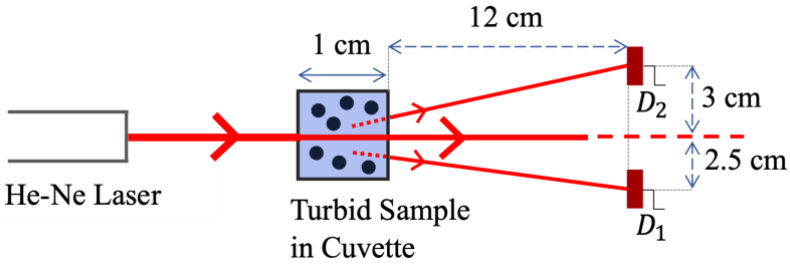

Fig 4. Schematic of the experimental setup to measure the scattered light at two angular positions at the detectors D_1 and D_2. The undeviated transmitted light is also measured (not shown) to determine the interaction coefficient μ_t.

As discussed in Sec 1, an important application of the Monte Carlo method is the determination of the scattering parameters of a turbid media, by comparing the experimental data with simulated results for different values of the scattering parameters. The experimental setup schematically shown in Fig 4 can be used to determine the size of particles in a turbid sample comprising polystyrene spheres [33]. Light from a He-Ne laser is incident normally on a cuvette containing the turbid sample, and the scattered light is measured at the two off-axis detectors D_1 and D_2, with circular apertures of diameters 2 mm and 1.1 mm, respectively. First, the undeviated transmitted light is used to estimate the interaction coefficient μ_t by using the Beer-Lambert law, and then the scattered light at the two detectors corresponding to different particle sizes is obtained from Monte Carlo simulations. The simulated curves for a medium with $\mu_t = 0.173$ cm^{-1} are shown in Fig 5. It can be seen that corresponding to the measurement at a single detector, the simulated scattered power matches with the measured power at two values of the particles size, one of which is the actual size of the particles in the given sample [11]. Similarly, another pair of possible particle sizes is obtained corresponding to the measurement at the other detector. Only one particle size is common to both pairs, which is identified as the correct size. Thus, by measuring the scattered powers at two angular positions, the size of the spherical particles can be uniquely determined.

The Monte Carlo method involves simulation of millions or billions of photon packets, which may be time consuming. When the simulations need to be performed for different values of the scattering parameters, scaling methods can be used, in which the simulation results corresponding to a few combinations of parameters can lead to the results for other combinations of parameters without performing the simulations again

[106–108]. If the scattering parameters vary gradually throughout the medium, then the initial simulations can be used to obtain the results by using the perturbation theory [109]; this is called the perturbation Monte Carlo method [110,111]. In some cases, hybrid Monte Carlo models can be used, in which the Monte Carlo method is combined with analytical methods, such as the diffusion approximation [34,112] and geometric ray tracing [113], in order to decrease the total simulation time without compromising the accuracy. Since each photon packet is propagated independently, the computation speed can also be drastically increased through the use of parallel computation techniques, in which the propagation of multiple packets is simulated simultaneously [114-117]. A detailed description of the different types of Monte Carlo techniques can be found in [118].

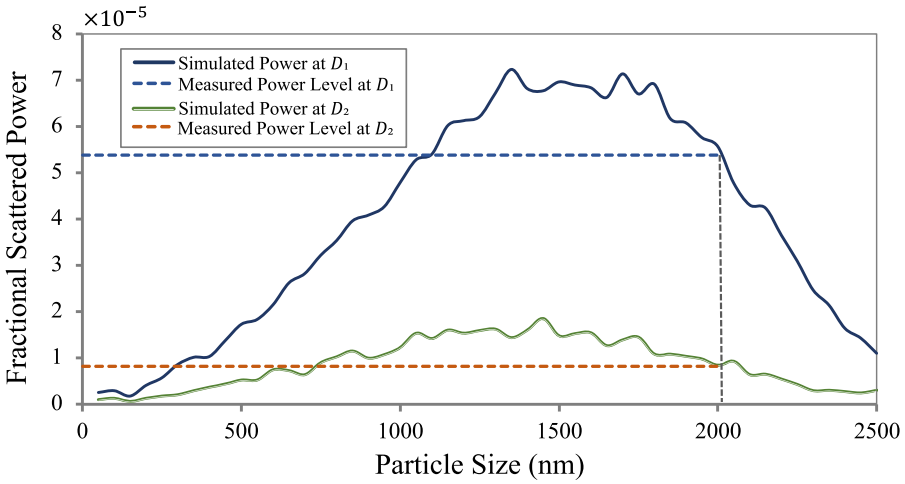

Fig 5. Simulated scattered power collected at detectors D_1 and D_2, for a turbid medium comprising polystyrene spheres with interaction coefficient $\mu_t = 0.173$ cm^{-1}. The particle size was changed in steps of 100 nm, and 10 million photon packets were simulated for each particle size. The experimentally obtained scattered powers corresponding to a sample with (actual) particle size = 2000 nm are shown with dotted lines. The measured power at a particular detector may correspond to the simulated power for more than one particle size, but only one particle size corresponds to the measured power levels at both the detectors.

As mentioned before, in the Monte Carlo model the photon packets are treated as classical entity. Wave effects like coherence [119] and polarization [43,120], which incorporate the Mueller matrix, can be included in the simulations as well, but these are rarely used since the polarization and phase information of the scattered light is usually lost due to multiple scattering and decoherence while propagating through a turbid medium. Over the past few years, variations in the Monte Carlo model have also been reported for applications to anisotropic (birefringent) media [121,122] and inhomogeneous scattering media [123,124], in which the medium is divided into voxels; 'voxel' refers to an infinitesimally small three dimensional region inside which the scattering parameters are assumed to be constant.

If a photon packet moves from one voxel to another, the remaining step size of the packet is scaled according to the scattering coefficients of the previous– and the current voxels, and the scattering angle after an interaction event is chosen according to $p(\theta)$ or g of the voxel inside which the scattering took place [125]. Monte Carlo simulations can also be performed for turbid mixtures, i.e., media which comprise more than one type of particles [126], by using equivalent scattering parameters which are the weighted average of the parameters for each type of particles, with the weights depending on their respective concentrations [127-130]. Equivalent scattering parameters, for example, can be used to model light propagation in a bidisperse mixture for the determination of the concentration of the two types of constituents in the mixture [126].

4 Conclusion

In this review, we have discussed various methods employed to determine the scattered light from particulate matter through analytical or numerical calculations. Almost all the methods are based on the solution of the Maxwell's equations, which dictate the light scattering phenomenon. The Mie theory, which gives analytical solution of the scattering problem for spherical particles, has been discussed in detail, followed by other approximate and numerical methods. We then extended our discussion to the case of multiple particles, i.e., a turbid (scattering) medium. The propagation of light inside a turbid medium can be modelled both analytically and through stochastic simulations, which form the basis of the radiative transfer equation (RTE) and the Monte Carlo method, respectively.

The inverse problem has become a focal topic of research in recent years due to its umpteen possibilities of practical applications, for both single particles and turbid media, whose properties can be determined by comparing the measured scattered power with that obtained from simulations or calculations for a variety of test parameters. Light scattering methodologies can also be 'inverted' for applications to cases where the effect of scattered light needs to be removed or minimized, e.g. in imaging of objects hidden inside a scattering medium [117,131,132], improving visibility in haze [133], and measurements on biological samples [134]. Further, light scattering calculations can also be used for optimization of the experimental setups [135], in terms of various factors such as sensitivity, dynamic range, and cost. The importance of simulations is also in the development and verification of analytical methods, where the 'experimental' data is obtained numerically in lieu of actual experiments [136-138]. Thus, calculations pertaining to the scattered light are intertwined with various light scattering techniques, and research is continuously ongoing with the aim of making the numerical predictions of light scattering studies faster, more accurate, and versatile.

Acknowledgement

Kalpak Gupta gratefully acknowledges financial support for this work through the award of a research fellowship by the University Grants Commission (UGC), India.

References

1. Campbell C G, Laycak D T, Hoppes W, Tran N T, Shi F G, High concentration suspended sediment measurements using a continuous fiber optic in-stream transmissometer, *J Hydrol*, 311(2005)244–253.
2. Osborne P D, Vincent C E, Greenwoodt B, Measurement of suspended sand concentrations in the nearshore: field intercomparison of optical and acoustic backscatter sensors, *Cont Shelf Res*, 14(1994)159–174.
3. Wren D G, Barkdoll B D, Kuhnle R A, Derrow R W, Field Techniques for Suspended-Sediment Measurement, *J Hydraul Eng*, 126(2000)97–104.
4. Inoue T, Sanpei A, Kawade Y, Suzuki M, Ochiai R, Awatsuji Y, Identification of Pollens From Polymer Particles Levitating in an RF Plasma by the Polarization Imaging Method, *IEEE Trans Plasma Sci*, 49(2021)2967–2971.
5. Nakayama T, Matsumi Y, Kawahito K, Watabe Y, Development and evaluation of a palm-sized optical $PM_{2.5}$ sensor, *Aerosol Sci Technol*, 52(2018)2–12.
6. Hyslop N P, Impaired visibility: the air pollution people see, *Atmos Environ*, 43(2009)182–195.
7. Volten H, Muñoz O, Rol E, de Haan J F, Vassen W, Hovenier J W, Muinonen K, Nousiainen T, Scattering matrices of mineral aerosol particles at 441.6 nm and 632.8 nm, *J Geophys Res Atmos*, 106(2001)17375–17401.
8. Kemppinen O, Nousiainen T, Merikallio S, Räisänen P, Retrieving microphysical properties of dust-like particles using ellipsoids: the case of refractive index, *Atmos Chem Phys*, 15(2015)11117–11132.
9. Bergmann F, Foschum F, Zuber R, Kienle A, Precise determination of the optical properties of turbid media using an optimized integrating sphere and advanced Monte Carlo simulations. Part 2: experiments, *Appl Opt*, 59(2020) 3216–3226.
10. Prerana, Shenoy M R, Pal B P, Method to determine the optical properties of turbid media, *Appl Opt*, 47(2008), 3216–3220.
11. Gupta K, Shenoy M R, Method to determine the anisotropy parameter *g* of a turbid medium, *Appl Opt*, 57(2018) 7559–7563.

12. Montrucchio B, Giusto E, Vakili M G, Quer S, Ferrero R, Fornaro C, A Densely-Deployed, High Sampling Rate, Open-Source Air Pollution Monitoring WSN, *IEEE Trans Veh Technol*, 69(2020)15786–15799.
13. Miki K, Fujita T, Sahashi N, Development and application of a method to classify airborne pollen taxa concentration using light scattering data, *Sci Rep*, 11(2021)22371; doi. 10.1038/s41598-021-01919-7.
14. Prerana, Shenoy M R, Pal B P, Gupta B D, Design, analysis, and realization of a turbidity sensor based on collection of scattered light by a fiber-optic probe, *IEEE Sens J*, 12(2012)44–50.
15. Shenoy M R, Optical fibre probes in the measurement of scattered light: Application for sensing turbidity, *Pramana -- J Phys*, 82(2014)39–48.
16. Huang J, Qian R, Gao J, Bing H, Huang Q, Qi L, Song S, Huang J, A novel framework to predict water turbidity using Bayesian modeling, *Water Res*, 202(2021)117406; doi. 10.1016/j.watres.2021.117406.
17. Miklos D B, Remy C, Jekel M, Linden K G, Drewes J E, Hübner U, Evaluation of advanced oxidation processes for water and wastewater treatment – A critical review, *Water Res*, 139(2018)118–131.
18. Wen Y, Mao Y, Wang X, Application of chromaticity coordinates for solution turbidity measurement, *Measurement*, 130(2018)39–43.
19. Gao Z L, Cheng Q D, Zeng G L, Wen Y, Li G F, Chen J, Dong Y B, Ji Q Z, Review of Calibration and Improvement Methods of Light- Scattering Airborne Particle Concentration, *J Phys: Conf Ser*, 2097(2021) 012008; doi. 10.1088/1742-6596/2097/1/012008.
20. Świrniak G, Mroczka J, Forward and inverse analysis for particle size distribution measurements of disperse samples: A review, *Measurement*, 187(2022) 110256; doi. 10.1016/j.measurement.2021.110256.
21. Wang H, Li J, Liao R, Tao Y, Peng L, Li H, Deng H, Ma H, Early warning of cyanobacterial blooms based on polarized light scattering powered by machine learning, *Measurement*, 184(2021) 109902; doi. 10.1016/j.measurement.2021.109902.
22. Selden A C, Attenuation and impulse response for multiple scattering of light in atmospheric clouds and aerosols, *Appl Opt*, 45(2006)3144–3151.
23. Ceolato R, Berg M J, Aerosol light extinction and backscattering: A review with a lidar perspective, *J Quant Spectrosc Radiat Transf*, 262(2021) 107492; doi.org/10.1016/j.jqsrt.2020.107492.
24. Ye Y, Pui D Y H, Detection of nanoparticles suspended in a light scattering medium, *Sci Rep*, 11(2021)20268; doi. 10.1038/s41598-021-99768-x.
25. Wax A, Yang C, Backman V, Kalashnikov M, Dasari R R, Feld M S, Determination of particle size by using the angular distribution of backscattered light as measured with low-coherence interferometry, *J Opt Soc Am A*, 19(2002)737–744.
26. Augsten C, Kiselev M A, Gehrke R, Hause G, Mäder K, A detailed analysis of biodegradable nanospheres by different techniques—A combined approach to detect particle sizes and size distributions, *J Pharm Biomed Anal*, 47(2008)95–102.
27. Wang R, Yu G, Suspended sediment concentration measurement based on optical fiber technology, *Meas Sci Technol*, 30(2019) 075205; doi. 10.1088/1361-6501/ab188d.
28. Lee B, Review of the present status of optical fiber sensors, *Opt Fiber Technol*, 9(2003)57–79.
29. Kerker M, The Scattering of Light and Other Electromagnetic Radiation, (Academic Press, Inc., New York), 1969.
30. Bal G, Inverse transport theory and applications, *Inverse Probl*, 25(2009) 053001; doi. 10.1088/0266-5611/25/5/053001.
31. Hulst H C van de, Light Scattering by Small Particles, (John Wiley & Sons, Inc., New York), 1957.
32. Bohren C F, Huffman D R, Absorption and Scattering of Light by Small Particles, (John Wiley & Sons, Inc., USA), 1983.
33. Gupta K, Shenoy M R, Compact setup to determine size and concentration of spherical particles in a turbid medium, *Appl Opt*, 60(2021)8174–8180.
34. Wang L V, Wu H, Biomedical Optics, (John Wiley & Sons, Inc., Hoboken, New Jersey), 2007.
35. Shenoy M R, Gupta K, Light Scattering by Turbid Media, *Asian J Phys*, 28(2019)1163–1173.
36. Marx E, Mulholland G W, Size and Refractive Index Determination of Single Polystyrene Spheres, *J Res Natl Bur Stand*, 88(1983)321–338.
37. Bell B W, Bickel W S, Single fiber light scattering matrix: an experimental determination, *Appl Opt*, 20(1981) 3874–3876.
38. Bartholdi M, Salzman G C, Hiebert R D, Kerker M, Differential light scattering photometer for rapid analysis of single particles in flow, *Appl Opt*, 19(1980)1573–1581.

39. Sloot P M A, Hoekstra A G, van der Liet H, Figdor C G, Scattering matrix elements of biological particles measured in a flow through system: theory and practice, *Appl Opt*, 28(1989)1752–1762.
40. Yastrebova E S, Litvinenko A L, Strokotov D I, Vladimirov R S, Gilev K V, Nekrasov V M, Karpenko A A, Maltsev V P, Dual-wavelength angle-resolved light scattering used in the analysis of particles by scanning flow cytometry, *J Opt*, 23(2021) 105606; doi. 10.1088/2040-8986/ac1b7b.
41. Friebel M, Roggan A, Müller G, Meinke M, Determination of optical properties of human blood in the spectral range 250 to 1100 nm using Monte Carlo simulations with hematocrit-dependent effective scattering phase functions, *J Biomed Opt*, 11(2006) 034021; doi. 10.1117/1.2203659
42. Liu F, Zhang S, Han P, Chen F, Zhao L, Fan Y, Shao X, Depolarization index from Mueller matrix descatters imaging in turbid water, *Chin Opt Lett*, 20(2022) 022601; doi.10.3788/COL202220.022601.
43. Bartel S, Hielscher A H, Monte Carlo simulations of the diffuse backscattering Mueller matrix for highly scattering media, *Appl Opt*, 39(2000)1580–1588.
44. Satapathi S, Soni J, Ghosh N, Fluorescent Mueller matrix analysis of a highly scattering turbid media, *Appl Phys Lett*, 104(2014) 131902; doi. 10.1063/1.4869475.
45. Gao W, Mueller matrix decomposition methods for tissue polarization tomography, *Opt Lasers Eng*, 147(2021) 106735; doi.10.1016/j.optlaseng.2021.106735.
46. Gonzalez M, Ossikovski R, Novikova T, Ramella-Roman J, Introduction of a 3×4 Mueller matrix decomposition method, *J Phys D: Appl Phys*, 54(2021) 424005; doi. 10.1088/1361-6463/ac1622.
47. Mie G, Beiträge zur Optik trüber Medien, speziell kolloidaler Metallösungen, *Ann Phys*, 330(1908)377–445.
48. Wiscombe W J, Improved Mie scattering algorithms, *Appl Opt*, 19(1980)1505–1509.
49. Laven P, MiePlot, *http://www.philiplaven.com/mieplot.htm*.
50. Sultanova N, Kasarova S, Nikolov I, Dispersion Properties of Optical Polymers, *Acta Phys Pol A*, 116(2009) 585–587.
51. Hale G M, Querry M R, Optical Constants of Water in the 200-nm to 200-µm Wavelength Region, *Appl Opt*, 12(1973)555–563.
52. Mishchenko M I, Travis L D, Light scattering by polydispersions of randomly oriented spheroids with sizes comparable to wavelengths of observation, *Appl Opt*, 33(1994)7206–7225.
53. Kodach V M, Faber D J, van Marle J, van Leeuwen T G, Kalkman J, Determination of the scattering anisotropy with optical coherence tomography, *Opt Express*, 19(2011)6131–6140.
54. Martin R J, Mie Scattering Formulae for Non-spherical Particles, *J Mod Opt*, 40(1993)2467–2494.
55. Aden A L, Kerker M, Scattering of Electromagnetic Waves from Two Concentric Spheres, *J Appl Phys*, 22(1951) 1242–1246.
56. Kaiser T, Schweiger G, Stable algorithm for the computation of Mie coefficients for scattered and transmitted fields of a coated sphere, *Comput Phys*, 7(1993)682–686.
57. Bohren C F, Light scattering by an optically active sphere, *Chem Phys Lett*, 29(1974)458–462.
58. Tang C, Auguié B, Le Ru E C, Modeling Molecular Orientation Effects in Dye-Coated Nanostructures using a Thin-Shell Approximation of Mie Theory for Radially Anisotropic Media, *ACS Photonics*, 5(2018)5002–5009.
59. Heinisch R L, Bronold F X, Fehske H, Mie Scattering by a Charged Dielectric Particle, *Phys Rev Lett*, 109(2012) 243903; doi. 10.1103/PhysRevLett.109.243903.
60. Wriedt T, A Review of Elastic Light Scattering Theories, *Part Part Syst Charact*, 15(1998)67–74.
61. Fu Q, Sun W, Mie theory for light scattering by a spherical particle in an absorbing medium, *Appl Opt*, 40(2001) 1354–1361.
62. Asano S, Yamamoto G, Light Scattering by a Spheroidal Particle, *Appl Opt*, 14(1975)29–49.
63. Tang C C H, Backscattering from Dielectric-Coated Infinite Cylindrical Obstacles, *J Appl Phys*, 28(1957)628–633.
64. Miles R B, Lempert W R, Forkey J N, Laser Rayleigh scattering, *Meas Sci Technol*, 12(2001)R33–R51.
65. Pang J, Baitenov A, Montanari C, Samanta A, Berglund L, Popov S, Zozoulenko I, Light Propagation in Transparent Wood: Efficient Ray-Tracing Simulation and Retrieving an Effective Refractive Index of Wood Scaffold, *Adv Photo Res*, 2(2021) 2100135; doi.10.1002/adpr.202100135.
66. Yee K S, Numerical solution of initial boundary value problems involving maxwell's equations in isotropic media, *IEEE Trans Antennas Propag*, 14(1966)302–307.

67. Taflove A, Hagness S C, Piket-May M, Computational Electromagnetics: The Finite-Difference Time-Domain Method, in The Electrical Engineering Handbook, (Academic Press), 2005, pp 629–670.
68. Drezek R, Dunn A, Richards-Kortum R, Light scattering from cells: finite-difference time-domain simulations and goniometric measurements, *Appl Opt*, 38(1999)3651–3661.
69. Schweiger M, Arridge S R, Hiraoka M, Delpy D T, The finite element method for the propagation of light in scattering media: Boundary and source conditions, *Med Phys*, 22(1995)779–1792.
70. Muinonen K, Markkanen J, Väisänen T, Peltoniemi J, Penttilä A, Multiple scattering of light in discrete random media using incoherent interactions, *Opt Lett*, 43(2018)683–686.
71. Schaubert D, Wilton D, Glisson A, A tetrahedral modeling method for electromagnetic scattering by arbitrarily shaped inhomogeneous dielectric bodies, *IEEE Trans Antennas Propagat*, 32(1984)77–85.
72. Draine B T, The discrete-dipole approximation and its application to interstellar graphite grains, *Astrophys J*, 333(1988)848–872.
73. Waterman P C, Symmetry, Unitarity, and Geometry in Electromagnetic Scattering, *Phys Rev D*, 3(1971)825–839.
74. Bi L, Yang P, Kattawar G W, Mishchenko M I, Efficient implementation of the invariant imbedding T-matrix method and the separation of variables method applied to large nonspherical inhomogeneous particles, *J Quant Spectrosc Radiat Transf*, 116(2013)169–183.
75. Mishchenko M I, Light scattering by randomly oriented axially symmetric particles, *J Opt Soc Am A*, 8(1991) 871–882.
76. Petrov D, Shkuratov Y, Zubko E, Videen G, *Sh*-matrices method as applied to scattering by particles with layered structure, *J Quant Spectrosc Radiat Transf*, 106(2007)437–454.
77. Somerville W R C, Auguié B, Le Ru E C, Accurate and convergent T-matrix calculations of light scattering by spheroids, *J Quant Spectrosc Radiat Transf*, 160(2015)29–35.
78. Mishchenko M I, Travis L D, Mackowski D W, T-matrix computations of light scattering by nonspherical particles: A review, *J Quant Spectrosc Radiat Transf*, 55(1996)535–575.
79. Harrington R F, Field computation by moment methods, (IEEE Press, Piscataway, NJ), 1993.
80. Purcell E M, Pennypacker C R, Scattering and Absorption of Light by Nonspherical Dielectric Grains, *Astrophys J*, 186(1973)705–714.
81. Bolt R A, ten Bosch J J, Method for measuring position-dependent volume reflection, *Appl Opt*, 32(1993)4641–4645.
82. Gandjbakhche A H, Weiss G H, Bonner R F, Nossal R, Photon path-length distributions for transmission through optically turbid slabs, *Phys Rev E*, 48(1993)810–818.
83. Xu M, Alfano R R, Random Walk of Polarized Light in Turbid Media, *Phys Rev Lett*, 95(2005)213901; doi. 10.1103/PhysRevLett.95.213901.
84. Svensson T, Vynck K, Grisi M, Savo R, Burresi M, Wiersma D S, Holey random walks: Optics of heterogeneous turbid composites, *Phys Rev E*, 87(2013) 022120; doi. 10.1103/PhysRevE.87.022120.
85. Liemert A, Kienle A, Novel analytical solution for the radiance in an anisotropically scattering medium, *Appl Opt*, 54(2015)1963–1969.
86. Groenhuis R A J, Ferwerda H A, Ten Bosch J J, Scattering and absorption of turbid materials determined from reflection measurements. 1: Theory, *Appl Opt*, 22(1983)2456–2462.
87. Venugopalan V, You J S, Tromberg B J, Radiative transport in the diffusion approximation: An extension for highly absorbing media and small source-detector separations, *Phys Rev E*, 58(1998)2395–2407.
88. Chin L C L, Whelan W M, Vitkin I A, Information content of point radiance measurements in turbid media: implications for interstitial optical property quantification, *Appl Opt*, 45(2006)2101–2114.
89. Liu L, Wan W, Li J, Zhao H, Gao F, Simultaneous recovery of a full set of optical properties in turbid media using incomplete P5 approximation to CW radiance, *Opt Lett*, 43(2018)4188–4191.
90. Meier R R, Lee J-S, Anderson D E, Atmospheric scattering of middle UV radiation from an internal source, *Appl Opt*, 17(1978)3216–3225.
91. Wang L, Jaques S L, Zheng L, MCML---Monte Carlo modeling of light transport in multi-layered Tissues, *Comput Methods Programs Biomed*, 47(1995)131–146.
92. Henyey L C, Greenstein J L, Diffuse radiation in the Galaxy, *Astrophys J*, 93(1941)70–83.

93. Cornette W M, Shanks J G, Physically reasonable analytic expression for the single-scattering phase function, *Appl Opt*, 31(1992)3152–3160.
94. Toublanc D, Henyey–Greenstein and Mie phase functions in Monte Carlo radiative transfer computations, *Appl Opt*, 35(1996)3270–3274.
95. Reynolds L O, McCormick N J, Approximate two-parameter phase function for light scattering, *J Opt Soc Am*, 70(1980)1206–1212.
96. Caton F, Baravian C, Mougel J, The influence of the microscopic characteristics of a random medium on incoherent light transport, *Opt Express*, 15(2007)2847–2872.
97. Vaudelle F, L'Huillier J-P, Askoura M L, Light source distribution and scattering phase function influence light transport in diffuse multi-layered media, *Opt Commun*, 392(2017)268–281.
98. Binzoni T, Leung T S, Gandjbakhche A H, Rüfenacht D, Delpy D T, The use of the Henyey–Greenstein phase function in Monte Carlo simulations in biomedical optics, *Phys Med Biol*, 51(2006, N313–N322.
99. Preston T C, Reid J P, Determining the size and refractive index of microspheres using the mode assignments from Mie resonances, *J Opt Soc Am A*, 32(2015)2210–2217.
100. Chu C-M, Churchill S W, Representation of the Angular Distribution of Radiation Scattered by a Spherical Particle, *J Opt Soc Am*, 45(1955)958–962.
101. Fowler B W, Expansion of Mie-theory phase functions in series of Legendre polynomials, *J Opt Soc Am*, 73(1983) 19–22.
102. Naglič P, Pernuš F, Likar B, Bürmen M, Lookup table-based sampling of the phase function for Monte Carlo simulations of light propagation in turbid media, *Biomed Opt Express*, 8(2017), 1895–1910.
103. Kattawar G W, A three-parameter analytic phase function for multiple scattering calculations, *J Quant Spectrosc Radiat Transf*, 15(1975)839–849.
104. Haltrin V I, One-parameter two-term Henyey-Greenstein phase function for light scattering in seawater, *Appl Opt*, 41(2002)1022–1028.
105. Liu Q, Weng F, Combined Henyey-Greenstein and Rayleigh phase function, *Appl Opt*, 45(2006)7475–7479.
106. Graaff R, Koelink M H, Mul F F M de, Zijlstra W G, Dassel A C M, Aarnoudse J G, Condensed Monte Carlo simulations for the description of light transport, *Appl Opt*, 32(1993)426–434.
107. Pifferi A, Taroni P, Valentini G, Andersson-Engels S, Real-time method for fitting time-resolved reflectance and transmittance measurements with a Monte Carlo model, *Appl Opt*, 37(1998)2774–2780.
108. Bevilacqua F, Depeursinge C, Monte Carlo study of diffuse reflectance at source–detector separations close to one transport mean free path, *J Opt Soc Am A*, 16(1999)2935–2945.
109. Ostermeyer M R, Jacques S L, Perturbation theory for diffuse light transport in complex biological tissues, *J Opt Soc Am A*, 14(1997)255–261.
110. Kumar Y P, Vasu R M, Reconstruction of optical properties of low-scattering tissue using derivative estimated through perturbation Monte-Carlo method, *J Biomed Opt*, 9(2004)1002–1012; doi.org/10.1117/1.1778733.
111. Hayakawa C K, Spanier J, Bevilacqua F, Dunn A K, You J S, Tromberg B J, Venugopalan V, Perturbation Monte Carlo methods to solve inverse photon migration problems in heterogeneous tissues, *Opt Lett*, 26(2001)1335–1337.
112. Wang L, Jacques S L, Hybrid model of Monte Carlo simulation and diffusion theory for light reflectance by turbid media, *J Opt Soc Am A*, 10(1993)1746–1752.
113. Lee S Y, Mycek M-A, Hybrid Monte Carlo simulation with ray tracing for fluorescence measurements in turbid media, *Opt Lett*, 43(2018)3846–3849.
114. Alerstam E, Svensson T, Andersson-Engels S, Parallel computing with graphics processing units for high-speed Monte Carlo simulation of photon migration, *J Biomed Opt*, 13(2008) 060504; doi. 10.1117/1.3041496.
115. Alerstam E, Lo W C Y, Han T D, Rose J, Andersson-Engels S, Lilge L, Next-generation acceleration and code optimization for light transport in turbid media using GPUs, *Biomed Opt Express*, 1(2010)658–675.
116. Fang Q, Boas D A, Monte Carlo Simulation of Photon Migration in 3D Turbid Media Accelerated by Graphics Processing Units, *Opt Express*, 17(2009)20178–20190.
117. Jönsson J, Berrocal E, *Multi-Scattering* software: part I: online accelerated Monte Carlo simulation of light transport through scattering media, *Opt Express*, 28(2020)37612–37638.

118. Zhu C, Liu Q, Review of Monte Carlo modeling of light transport in tissues, *J Biomed Opt*, 18(2013) 050902; doi. 10.1117/1.JBO.18.5.050902.
119. Shen Z, Sukhov S, Dogariu A, Monte Carlo method to model optical coherence propagation in random media, *J Opt Soc Am A*, 34(2017)2189–2193.
120. Kaplan B, Ledanois G, Drévillon B, Mueller matrix of dense polystyrene latex sphere suspensions: measurements and Monte Carlo simulation, *Appl Opt*, 40(2001)2769–2777.
121. Wang X, Wang L V, Propagation of polarized light in birefringent turbid media: A Monte Carlo study, *J Biomed Opt*, 7(2002) 279; doi. 10.1117/1.1483315.
122. Côté D, Vitkin I A, Robust concentration determination of optically active molecules in turbid media with validated three-dimensional polarization sensitive Monte Carlo calculations, *Opt Express*, 13(2005)148–163.
123. Kumar A T N, Direct Monte Carlo computation of time-resolved fluorescence in heterogeneous turbid media, *Opt Lett*, 37(2012)4783–4785.
124. Pavlov M S, Krasnikov I V, Seteĭkin A Yu, Monte Carlo modelling of optical-radiation propagation in biological media with closed internal inhomogeneities, *J Opt Technol*, 77(2010)602–605.
125. Boas D A, Culver J P, Stott J J, Dunn A K, Three dimensional Monte Carlo code for photon migration through complex heterogeneous media including the adult human head, *Opt Express*, 10(2002)159–170.
126. Gupta K, Shenoy M R, Method to determine the concentrations of constituents in a bidisperse turbid medium using Monte Carlo simulation for mixtures, *OSA Continuum*, 4(2021)2232–2244.
127. Meglinskii I V, Monte Carlo simulation of reflection spectra of random multilayer media strongly scattering and absorbing light, *Quantum Electron*, 31(2001)1101–1107.
128. Sharma S K, Banerjee S, Role of approximate phase functions in Monte Carlo simulation of light propagation in tissues, *J Opt A: Pure Appl Opt*, 5(2003)294–302.
129. Meglinski I V, Matcher S J, Computer simulation of the skin reflectance spectra, *Comput Methods Programs Biomed*, 70(2003)179–186.
130. Gélébart B, Tinet E, Tualle J M, Avrillier S, Phase function simulation in tissue phantoms: a fractal approach, *Pure Appl Opt*, 5(1996)377–388.
131. Katz O, Small E, Guan Y, Silberberg Y, Noninvasive nonlinear focusing and imaging through strongly scattering turbid layers, *Optica*, 1(2014)170–174.
132. Wang H, Li J, Hu H, Jiang J, Li X, Zhao K, Cheng Z, Sang M, Liu T, Underwater imaging by suppressing the backscattered light based on Mueller matrix, *IEEE Photonics J*, 13(2021) 7800106; doi.10.1109/JPHOT.2021.3094359.
133. Guo L, Cui Y, He Q, Gao W, Pei K, Zhu L, Li H, Wang X, Contributions of aerosol chemical composition and sources to light extinction during haze and non-haze days in Taiyuan, China, *Atmos Pollut Res*, 12(2021) 101140; doi. 10.1016/j.apr.2021.101140.
134. Awelisah Y M, Li G, Wang Y, Tang W, Lin L, Considering blood scattering effect in noninvasive optical detection of blood components using dynamic spectrum along with time varying filter based empirical mode decomposition, *Biomed Signal Process Control*, 71(2022) 103266; doi. 10.1016/j.bspc.2021.103266.
135. Foschum F, Bergmann F, Kienle A, Precise determination of the optical properties of turbid media using an optimized integrating sphere and advanced Monte Carlo simulations Part 1: theory, *Appl Opt*, 59(2020)3203–3215.
136. Menon S, Su Q, Grobe R, Determination of g and μ using Multiply Scattered Light in Turbid Media, *Phys Rev Lett*, 94(2005) 153904; doi.10.1103/PhysRevLett.94.153904.
137. Penttilä A, Zubko E, Lumme K, Muinonen K, Yurkin M A, Draine B, Rahola J, Hoekstra A G, Shkuratov Y, Comparison between discrete dipole implementations and exact techniques, *J Quant Spectrosc Radiat Transf*, 106(2007)417–436.
138. Menon S, Su Q, Grobe R, Comparison of the Maxwell and Boltzmann theory for multilayered dielectric random media, *Phys Rev E*, 65(2002) 051917; doi. 10.1103/PhysRevE.65.051917.

[*Received*: 01.12. 2021; *Revised Recd*: 13.01.2022; *accepted*: 01.03.2022]